Separation Science and Technology
Publication details, including instructions for authors and subscription information:
http://www.informaworld.com/smpp/title~content=t713708471

Non-Isothermal Non-Adiabatic Dehydrogenation of Cyclohexane in Catalytic Membrane Reactors

Mohamed Al-Sahali[a]; Hisham M. Ettouney[a]; Bader Albusairi[a]; Haitham Lababidi[a]; Heba A. Al-Hulaila[a]
[a] Department of Chemical Engineering, College of Engineering and Petroleum-Kuwait University, Safat, Kuwait

To cite this Article Al-Sahali, Mohamed , Ettouney, Hisham M. , Albusairi, Bader , Lababidi, Haitham and Al-Hulaila, Heba A.(2007) 'Non-Isothermal Non-Adiabatic Dehydrogenation of Cyclohexane in Catalytic Membrane Reactors', Separation Science and Technology, 42: 9, 2081 — 2097
To link to this Article: DOI: 10.1080/01496390701242020
URL: http://dx.doi.org/10.1080/01496390701242020

Separation Science and Technology, 42: 2081–2097, 2007

ISSN 0149-6395 print/1520-5754 online
DOI: 10.1080/01496390701242020

Non-Isothermal Non-Adiabatic Dehydrogenation of Cyclohexane in Catalytic Membrane Reactors

Mohamed Al-Sahali, Hisham M. Ettouney, Bader Albusairi, Haitham Lababidi, and Heba A. Al-Hulaila
Department of Chemical Engineering, College of Engineering and Petroleum–Kuwait University, Safat, Kuwait

Abstract: This study focuses on modeling and analysis of the non-isothermal, non-adiabatic, dehydrogenation of cyclohexane in membrane catalytic reactors. The dehydrogenation reaction is endothermic with a low equilibrium conversion of 0.06 at a temperature of 473 K and pressure of 101 kPa. The membrane reactor removes hydrogen from the reaction mixture and results in increase of the reaction conversion. The analysis is made as a function of feed flow rate, feed temperature, feed composition, inert flow rate in the feed stream, flow rate of sweep gas, pressures of the tube side and shell side, permeability constant of hydrogen, and tube diameter. The analysis also includes a study of the co-current and the counter-current flow modes. The results show lower conversion for the counter-current flow mode, because of the decrease in the driving force for permeation. A comparison of model predictions against previous literature studies shows good agreement.

Keywords: Membrane reactors, ceramic and metallic membranes, catalytic reactors, dehydrogenation, modeling

INTRODUCTION

Membrane catalytic reactors remain to be found on a limited scale in industrial applications. This is because of the large cost involved in modification

Received 31 August 2006, Accepted 17 January 2007
Address correspondence to Hisham M. Ettouney, Department of Chemical Engineering, College of Engineering and Petroleum–Kuwait University, P. O. Box 5969, Safat 13060, Kuwait. Tel.: 965-4985619; Fax: 965-4839498; E-mail: ettouney@hotmail.com

of existing industrial processes. Also, a huge field of experience has been accumulated for design, construction, operation, and maintenance of the more conventional fixed bed configuration. Irrespective of this, membrane catalytic reactors are highly valuable for low conversion equilibrium reactions. This is because removing part of the reaction products would shift the reaction equilibrium to higher conversion and yield rates, which might offset the cost and higher risks of adopting a new technology. Literature review shows a large number of mathematical and experimental evaluation of catalytic membrane reactors. Most of these systems are used for dehydrogenation reactions where a thick or composite metallic membrane (palladium or platinum) is used for removal of hydrogen from the reaction mixture. Metallic membranes are more selective than the less expensive glass or ceramic membranes. Other applications of membrane reactors include oxidation, decomposition, and isomerization. Most of the studies employ a double pipe configuration, where the catalyst is kept on the shell side and the permeate flows across the tube side membrane. Sweep/inert gas is used on the tube side to aid in the removal of the permeate gas. In addition, the use of a sweep gas would reduce the mole fraction of the permeating species, which in turn increases the driving forces for permeation across the membrane.

Itoh (1) used a thick palladium membrane, 200 μm, which permeates only hydrogen. At a temperature of 473 K, the cyclohexane conversion for the membrane configuration is measured at 99.7%. At this temperature, the equilibrium conversion is limited to 18.7%. Itoh et al. (2) used a microporous glass membrane, which is less selective and less expensive than thick palladium membranes, to study cyclohexane dehydrogenation. The main merit of the microporous membrane is its low cost in comparison with thick palladium tubes. Also, the microporous membranes can increase the cyclohexane conversion by a factor of two. Itoh and Wu (3) tested the performance of a thick palladium membrane reactor, where cyclohexane dehydrogenation occurs on the tube side and hydrogen oxidation occurs on the shell side. This scheme is found to increase conversion by a factor of two over the case of the membrane reactor with inert sweep gas and a factor of four for a fixed bed configuration. Recently, Itoh et al. (4) tested a thin palladium membrane (4 μm) supported on a porous ceramic tube. The membrane is used for dehydrogenation of cyclohexane. The results show comparable performance to the thick palladium tube. However, thin membranes provide lower permeation resistance, which results in the increase of the production rate. Okubo et al. (5) showed similar results upon the use of 4 μm membrane supported on a ceramic tube. Jeong et al. (6) studied the performance of the zeolite type membrane for simultaneous removal of hydrogen and benzene. At 473 K, adjustment of the sweep gas and cyclohexane feed flow rate gave a conversion of 72% for the membrane reactor versus 32.2% for the fixed bed configuration.

Kokugan et al. (7) studied cyclohexane dehydrogenation using three types of membranes, which includes porous vycor glass, ceramic, and a thin layer of palladium silver. The high selectivity of the palladium silver membrane provided the highest conversions. Tiscareno-Lechuga et al. (8) studied cyclohexane dehydrogenation in three configurations which includes a fixed bed, a membrane reactor, and a hybrid reactor. The hybrid reactor is formed of two parts; upstream is the fixed bed part and downstream is the membrane part. The membrane and hybrid reactors remove part of the reaction products and permeate the inert sweep gas from the shell side to the tube side. This last effect also dilutes the reaction mixtures and results in equilibrium shift to higher conversions. The concept of hybrid reactor is similar to the two configurations proposed previously by Ettouney et al. (9) for an analysis of the high temperature CO shift conversion. The configurations include the membrane reactor and fixed bed reactor with separate inert membrane separation elements. The results show that use of the combined system of a fixed bed reactor and non-reactive membrane separation is more efficient than the membrane reactor because it gives a higher conversion with the least amount of catalyst.

Other applications of membrane catalytic reactors include dehydrogenation of ethyl benzene to styrene (10), methane steam reforming (11), dehydrogenation of isobutene (12), propane oxidation to acrolein (13), oxidation of n-butane to maleic anhydride (14), ammonia decomposition (15), and hydrogen sulfide decomposition (16). In summary, the above studies searched for an inexpensive, selective, and high permeability membrane that would result in the highest possible reaction conversion. A number of reactor configurations are tested; the most common is the double pipe configuration. Other reactor configurations include hybrids of a fixed-bed, membrane reactor, and inert membrane separation.

This study models the cyclohexane dehydrogenation for non-isothermal and adiabatic/non-adiabatic conditions. Also, the model considers co-current and counter-current operating modes. Cyclohexane is an excellent hydrogen carrier with high hydrogen content (7.1 wt%) (4). The dehydrogenation product, benzene, can be recycled and hydrogenated. The above literature review shows that cyclohexane dehydrogenation in membrane reactors is well studied; however, most of these studies are performed for the co-current flow mode and isothermal operation (1–7, 18–21).

MODEL ASSUMPTIONS AND EQUATIONS

A steady state plug flow model is developed for simulation of cyclohexane dehydrogenation in a membrane reactor, Fig. 1. The main model assumption is steady state operation, which is the industrial standard. Most of industrial applications focess on maintaining constant production rates. Therefore, prolonged operation may call for increase in the reactor temperature,

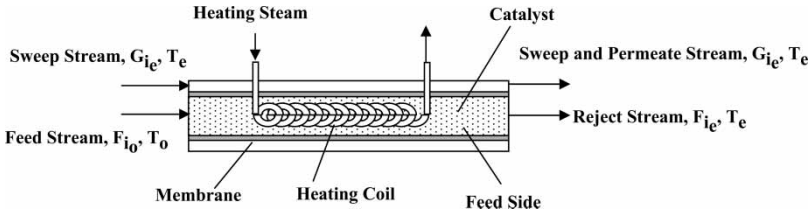

Figure 1. Schematic of membrane catalytic reactor with heating coil.

heating rate, catalyst regeneration, or partial replacement of the catalyst. This is to take into account the continuous decrease in the production rates due to catalyst fouling, deactivation, and poisoning. The model assumes a negligible pressure drop along the tube or shell length. The membrane considered in the model is assumed catalytically inactive and only permeable to hydrogen. This is the case of thick or thin palladium membranes. Based on the above literature review use of the thin palladium membrane supported on porous ceramic tubes is favored. This configuration provides the highest permeation and production rates. The model takes into considerations axial variations in the gas temperature on the tube and shell sides; however, radial variations are assumed negligible. The temperature on the tube side is affected by the endothermic nature of the reaction and the heat added from the heating coil. The reactor configuration is assumed to be perfectly insulated from the surroundings. Therefore, heat losses from the shell side to the surroundings are negligible. Side reactions are assumed negligible; therefore, only the cyclohexane dehydrogenation reaction is considered, which is given by

$$C_6H_{12} \Leftrightarrow C_6H_6 + 3H_2$$

The reaction rate and rate constants reported by Itoh (1) are given by the following expressions:

$$r_C = -\frac{k(K_p\, p_C/\, p_H^3 - p_B)}{1 + (K_B K_p\, p_C/\, p_H^3)}$$

$$K_B = 2.03 \times 10^{-10} \exp\left(\frac{6270}{T}\right)$$

$$K_p = 4.89 \times 10^{35} \exp\left(\frac{3190}{T}\right)$$

$$k = 0.221 \exp\left(-\frac{4270}{T}\right)$$

The material balance equations include the tube side balances for cyclohexane, hydrogen, and benzene, which are given by

$$\frac{dF_C}{dV} = r_C \tag{1}$$

$$\frac{dF_H}{dV} = -3r_C - (4/D)\alpha_H(p_{H_t}^{0.5} - p_{H_s}^{0.5}) \tag{2}$$

$$F_B = F_{B_o} + F_{C_o} - F_C \tag{3}$$

Since, hydrogen is the only permeating species, the material balance on the shell side is written only for hydrogen

$$G_H = F_{H_o} + G_{H_o} + 3(F_{C_o} - F_C) - F_H \tag{4}$$

The energy balance equation is written for the tube side of the reactor

$$\sum_{i=1}^{m} F_i Cp_i \frac{dT}{dV} = r_C(-\Delta H_C) + q \tag{5}$$

Where

$$(-\Delta H_C) = -206.2\text{kJ/kmole}$$

$$Cp_C = 0.09414 + 4.962H10^{-4}\ T - 3.19H10^{-7}\ T^2 + 6.866H10^{-11}\ T^3$$

$$Cp_B = 0.07406 + 3.295H10^{-4}\ T - 2.52H10^{-7}\ T^2 + 7.757H10^{-11}\ T^3.$$

$$Cp_H = 0.02884 + 7.65H10^{-8}\ T + 3.288H10^{-9}\ T^2 - 8.698H10^{-13}\ T^3.$$

Gobina and Hughes (17) gave the following expression for the permeability constant of hydrogen permeation through a thin layer of Pd-23wt%Ag of 6 μm thickness on porous vycor glass

$$\alpha_H = \frac{1.006 \times 10^{-9}\ \exp(-767.343/T)}{\delta}$$

where T is the absolute reaction temperature (K), and δ is the membrane thickness (m).

SOLUTION ALGORITHM

The model equations constitute a system of first order, nonlinear, ordinary differential equations. The equations set is solved using the fourth order Runge-Kutta method. Prior to integration of the model equations, it is necessary to define the following parameters; which includes flow mode (co-current or counter-current); feed flow rate of each component on the tube sides; flow rate and composition of the sweep gas on the shell side; feed temperature; tube diameter; pressure on the tube and shell sides; and

heating load. Definition of the above parameter set would result in construction of the model equations and initial conditions. This would allow for numerical integration of the model equations and would generate the species and temperature profiles on the tube and shell side.

Equations (1), (2), and (5) are solved subject to the following boundary conditions, which are defined at $V = 0$ (or the reactor entrance) and applies for co-current flow:

$$F_i = F_{i_o} \tag{6}$$

$$G_i = G_{i_o} \tag{7}$$

$$T = T_o \tag{8}$$

Equations (6) and (8) still apply for counter-current flow and are also defined at $V = 0$. However, Eq. (7) applies at the other end of the reactor or $V = V_t$. Therefore, an estimate is made for G_{i_e} or the molar flow rates for all species at $V = 0$. This guess is varied until the values given by Eq. (5) are satisfied.

RESULTS AND DISCUSSION

An analysis of the reactor performance for cyclohexane dehydrogenation is shown in Figs. 2–10. The analysis includes variations in the cyclohexane conversion and the outlet reactor temperature as a function of the following parameters; feed flow rate, feed composition, sweep gas flow rate, inlet temperature, tube pressure, shell pressure, permeation constant, tube diameter, heat load, and reactor volume. All calculations are made at the following conditions; co-current flow; feed flow rate of 1×10^{-3} mole/s; feed composition of 100% cyclohexane; sweep flow rate of 0.1 mole/s; inlet temperature of

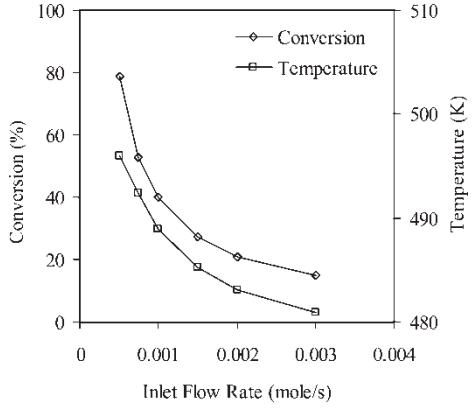

Figure 2. Variation in outlet cyclohexane conversion and reactor temperature as a function of the inlet feed flow rate.

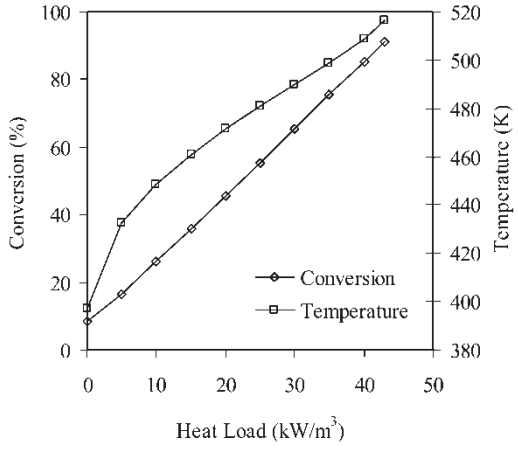

Figure 3. Variation in outlet cyclohexane conversion and reactor temperature as a function of the heating load of the reactor.

500 K; tube pressure of 200 kPa; shell pressure of 101 kPa; permeation constant of 0.00016767 mole/(kPa$^{0.5}$ s m^2); tube diameter of 0.016 m; and heating load of 43 kW/m^3. The reactor volume was adjusted for each set of calculations in order to achieve the maximum possible conversion. Values of the reactor volume are stated for each set of calculations.

Figure 2 shows variations in the outlet conversion and temperature as a function of the inlet flow rate. In these calculations, the inlet flow rate of cyclohexane is varied from 5×10^{-4} to 3×10^{-3} mole/s and the reactor volume is kept constant at 1.87×10^{-3} m^3. As is shown the cyclohexane conversion

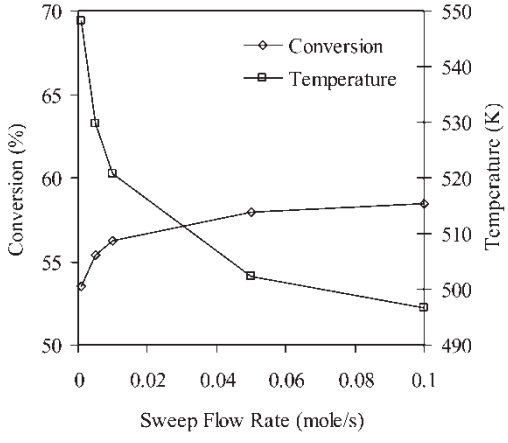

Figure 4. Variation in the outlet cyclohexane conversion and reactor temperature as a function of the sweep gas flow rate.

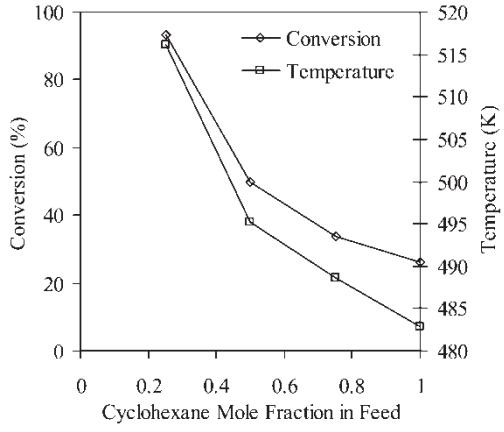

Figure 5. Variation in the outlet cyclohexane conversion and reactor temperature as a function of the cyclohexane mole fraction in the feed stream.

decreases with the increase in the flow rate. This is because of the decrease in the residence time of the reactants. The decrease in the outlet temperature is caused by the increase in the total feed flow rate. Selection of the optimum feed flow rate depends on the process economics and desired product flow rate. Operation at a low feed flow rate would result in a high conversion rate at the expense of a very low product flow rate. On the other hand, increasing the feed flow rate would reduce the conversion. This would require use of an extensive product separation system in order to recover the un-reacted feed.

Variations in the outlet conversion and temperature as a function of the heating load are shown in Fig. 3. The heating load is varied from 0 to 43

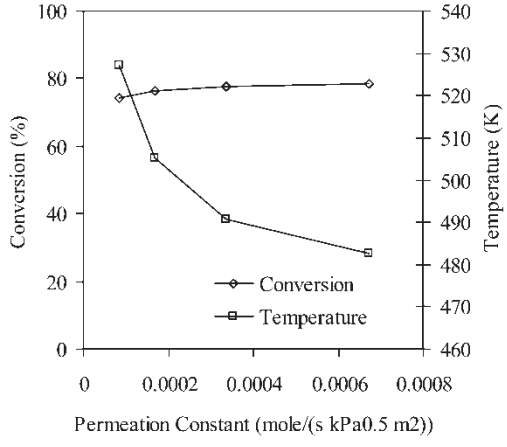

Figure 6. Variation in the outlet cyclohexane conversion and reactor temperature as a function of the hydrogen permeation constant.

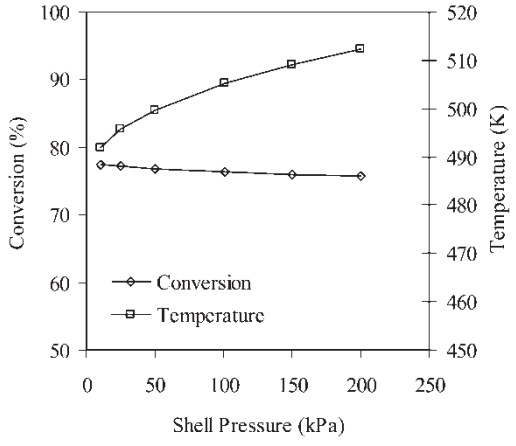

Figure 7. Variation in outlet cyclohexane conversion and reactor temperature as a function of shell pressure.

kW/m^3 and the reactor volume is kept constant at 4.42×10^{-3} m^3. Increasing the heating load increases the outlet conversion and temperature. The conversion increases linearly with the heating load. At high conversions, the major part of the heat supplied to the reactor is consumed by the endothermic reaction. On the other hand, at low conversions, a larger part of the heat added to the reactor is used to increase the temperature of the reaction mixture.

The effect of the sweep gas flow rate on the reaction conversion and the reactor temperature is shown in Fig. 4. The sweep gas flow rate is varied from 0 to 0.1 mole/s and the reactor volume is kept constant at 2.78×10^{-3} m^3.

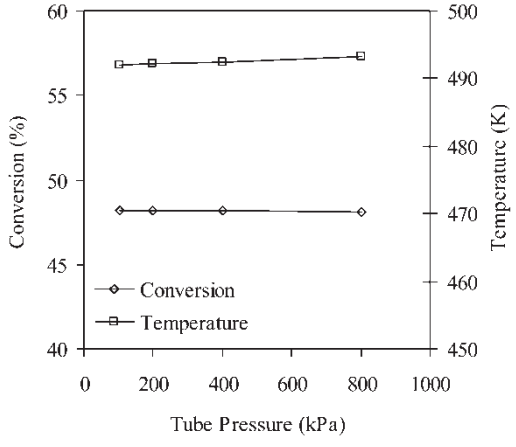

Figure 8. Variation in outlet cyclohexane conversion and reactor temperature as a function of the tube pressure.

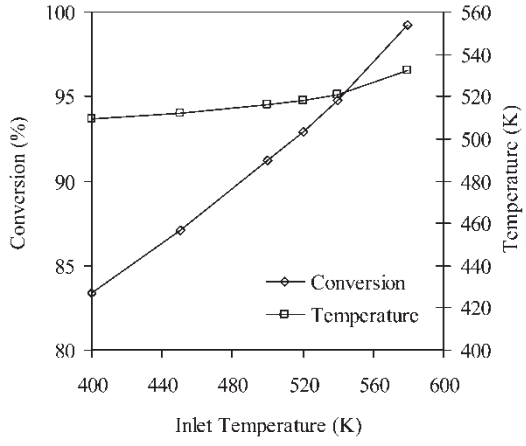

Figure 9. Variation in outlet cyclohexane conversion and reactor temperature as a function of the inlet temperature.

As is shown, increasing the sweep gas flow rate increases the reaction conversion and reduces the reactor temperature. Increasing the reaction conversion is caused by increasing the driving force for hydrogen permeation across the membrane, which causes a larger shift from equilibrium. As shown in

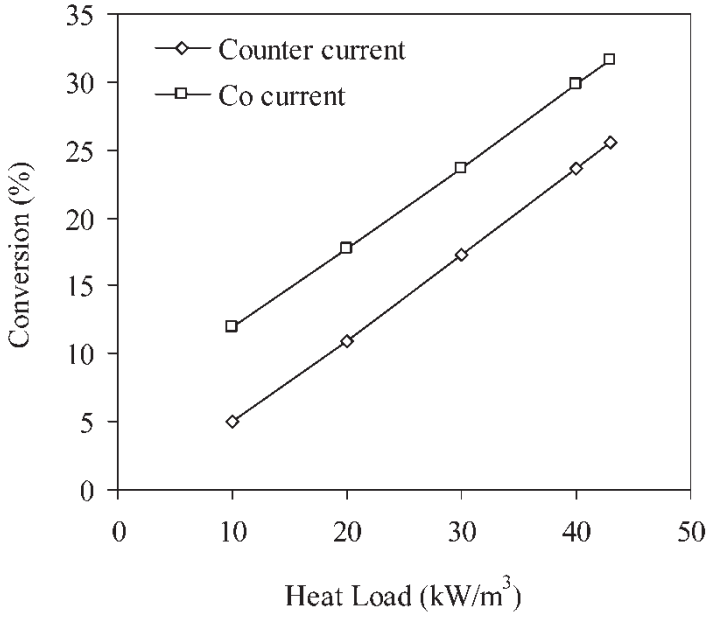

Figure 10. Variation in outlet cyclohexane conversion and reactor temperature as a function of the tube diameter.

Fig. 4, the conversion and reactor temperature rapidly approaches a plateau as the sweep gas flow rate reaches a value of 0.1 mole/s. At this condition, the mole fraction of the hydrogen permeate on the shell side is almost zero. Therefore, further increase in the sweep gas flow rate has a minimal effect on the reactor temperature and conversion.

Effect of the cyclohexane mole fraction in the feed stream is displayed in Fig. 5. The mole fraction of cyclohexane is varied from 25% up to 100% with benzene as the remaining balance. The reactor volume is kept constant at 1.17×10^{-3} m^3. as is shown, and an increase in the cyclohexane mole fraction in the feed stream decreases the outlet conversion and temperature. This is because increasing the cyclohexane mole fraction in the feed stream implies an increase in its feed flow rate and reduction in its residence time. Therefore, the conversion of cyclohexane decreases as its mole fraction increases in the feed stream. The decrease in the outlet temperature is caused by the increase in the specific heat of the feed stream. The presence of benzene in the feed stream has some effect on the conversion of cyclohexane, especially at small percentages for cyclohexane in the feed stream. For example, at a feed mole fraction of 0.25 of cyclohexane and the balance is benzene, the cyclohexane conversion is 93%. At the same conditions and replacement of benzene with inert increases, the conversion is a value close to 100%. The benzene effect on the cyclohexane conversion is reduced as the mole fraction of cyclohexane is reduced in the feed stream.

The effect of hydrogen permeation constant on the outlet conversion of cyclohexane and reactor temperature is shown in Fig. 6. The hydrogen permeation constant is varied from 8.38×10^{-5} mole/s up to 6.71×10^{-4} mole/s and the reactor volume is kept constant at 3.67×10^{-3} m^3. In actual practice this constant can be changed by altering the membrane properties, i.e., use of thick palladium or platinum tubes versus use of impregnated alumina tube. As is shown, the cyclohexane conversion increases to a value of 78% at a permeation constant of 6.71×10^{-4} mole/s. Simultaneously, the reactor temperature decreases due to the increase in the reaction rate. Increase in the hydrogen permeation constant results in the increase of the removal rate of hydrogen. This in turn shifts the reaction equilibrium to higher conversion rates.

The effects of the shell pressure on the outlet cyclohexane conversion and reactor temperature are shown in Fig. 7. In these calculations, the shell pressure is varied over a range of 10–200 kPa and the reactor volume is kept constant at 3.67×10^{-3} m^3. Similar to the results shown in Fig. 6, the cyclohexane conversion varies over a narrow range as the shell is increased, where the cyclohexane conversion is decreased from 77% to 75%. The decrease in the cyclohexane conversion is caused by the reduction in the driving for hydrogen permeation. This would increase the hydrogen mole fraction on the tube sides thus reducing the equilibrium shift to lower conversion. Simultaneously, the outlet reactor temperature would increase because of the reduction in the total amount of endothermic heat.

The effect of the feed or tube pressure on the outlet cyclohexane conversion and the reactor temperature is shown in Fig. 8. In these calculations, the tube pressure is varied from 101.3–800 kPa and the reactor volume is kept constant at 2.27×10^{-3} m^3. As is shown, the outlet cyclohexane conversion and reactor temperature have negligible dependence on this parameter. This is because increasing the pressure shifts the equilibrium to lower conversion. This is caused by the increase in the number of moles upon reaction. On the other hand, increasing the tube pressure increases the driving force for hydrogen permeation. This effect shifts the equilibrium to a higher conversion. The tube pressure effect is more evident at zero permeation constant, where the conversion decreases from 43.7% to 36.7% as the pressure is increased from 100 to 800 kPa.

Variations in the cyclohexane conversion and the reactor outlet temperature as a function of the feed temperature are shown in Fig. 9. The feed temperature is varied from 400–580 K and the reactor volume is kept constant at 3.16×10^{-3} m^3. As is shown, the outlet conversion and temperature are extremely sensitive to variations in the feed temperature. As is shown, the outlet cyclohexane conversion is increased from 83% up to 99%. Similarly, the outlet reactor temperature is increased from 509 K to 532 K. The increase in the outlet conversion is caused by the increase in the hydrogen permeation constant and the increase in the reaction rate at higher temperatures.

The effects of the tube diameter on the outlet conversion of cyclohexane and reactor temperature are shown in Fig. 10. In these calculations, the tube diameter is varied from 0.005–0.1 m and the reactor volume is kept constant at 4.42×10^{-3} m^3. As is shown, the conversion and temperature are very sensitive to variations in this parameter. The outlet conversion is decreased from 93% down to 86% and the temperature is increased from 495 K to 559 K. The decrease in the conversion is caused by the reduction in the permeation area upon the increase in the tube diameter. This in turn increases the resistance for hydrogen permeation. This would reduce the equilibrium shift and the cyclohexane conversion. The increase in the reactor temperature is caused by the decrease in the reaction rate due to low hydrogen removal from the reaction mixture.

Mass and heat transfer unit operations operated in counter current flow mode are characterized by a constant driving force for mass and heat transfer. This is illustrated in heat exchangers, where the logarithmic mean temperature difference remains constant along the length of the exchanger. On the other hand, a co-current heat exchanger would have a decreasing driving force. This results in a higher heat transfer area than the countercurrent flow mode. In non-reactive membrane separation processes, the countercurrent mode of operation is also more efficient than the co-current flow mode. Therefore, for the same membrane area a higher recovery and purity are achieved in the countercurrent flow mode. For reactive membrane systems, chemical reaction and equilibrium limitations reduces the efficiency of the countercurrent flow mode. At one end of the membrane reactor, where

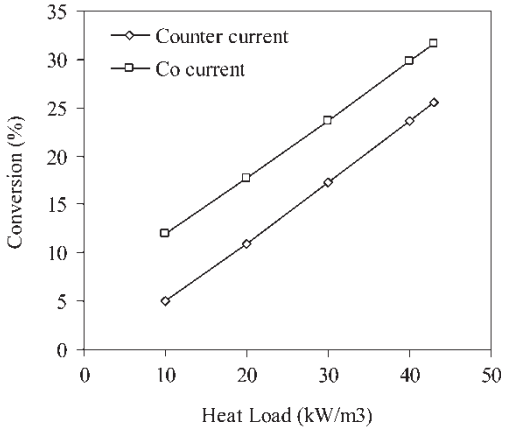

Figure 11. Variations in the outlet conversion as a function of heating load for co-current and counter current flow modes.

the feed is introduced and the permeate stream leaves the system, the driving force for hydrogen permeation would be lower than that for the co-current system. This is because of the high concentration of hydrogen on the permeate side in the countercurrent flow. At the other end for the countercurrent flow, where the feed stream leaves the system and the purge gas enters, the driving force for hydrogen permeation is higher than that for the co-current flow. However, this increase is offset by the low concentration of the reacting species, which would reduce the reaction rate. A comparison of the co-current and countercurrent flow modes is shown in Figs. 11–12. The

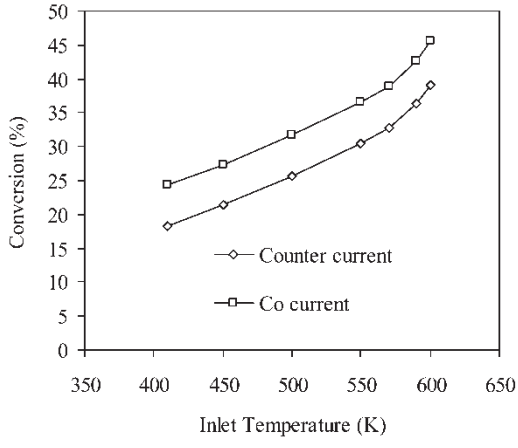

Figure 12. Variations in the outlet conversion as a function of the inlet temperature for co-current and counter current flow modes.

analysis is presented in terms of variations of the outlet reactor conversion as a function of the heating load and inlet temperature. As is shown the co-current mode of operation provides higher conversion than the counter current flow mode.

A comparison of the predictions of the model developed in this study against some of the above literature studies is shown in Table 1. The table shows experimental and model predictions for cyclohexane conversion. These values are shown for equilibrium conditions and for the membrane reactor. The data reported by Itoh (4) includes the tube diameter, tube length, feed flow rate, and feed composition. Achieving a good fit between model prediction and reported data required an adjustment of the feed flow

Table 1. Summary of comparison of model predictions against literature data. Values in parentheses correspond to experimental values

Reference	Itoh et al. (4)	Sun and Khang (21)	Kokugan et al. (7)
Membrane	4 μm Palladium membrane on α-alumina tube	Porous Vycor glass	Palladium – Silver
Catalyst	0.5 wt% Pt/Al_2O_3 pellets.	Pt within pores of the membrane (34 wt% Pt).	0.5 wt%Pt/Al_2O_3 pellets.
Operating conditions	Isothermal Co-Current	Isothermal Co-Current	Isothermal Co-Current
Temperature (K)	571 (571)	560 (560)	517 (473)
Tube pressure (kPa)	250 (250)	191 (191)	100 (100)
Permeation constant (mole/((kPa)$^{0.5}$ s m^2))	1×10^{-4} (NA)	1.02×10^{-5} (NA)	1×10^{-4} (NA)
Feed composition	100% Cyclohexane	Cyclohexane 50% (50%) Hydrogen 50% (50%) Benzene 0% (0%)	100% Cyclohexane
Feed flow rate (mole/s)	6.7×10^{-8} (5.8×10^{-8})	2.5×10^{-6} (2.5×10^{-6})	1×10^{-4} (1×10^{-4})
Sweep gas flow rate (mole/s)	0 (0)	0 (0)	0 (0)
Tube diameter (m)	0.00935 ($\sim$0.00935)	0.00796 (0.00796)	0.026 (0.026)
Reactor volume (m^3)	3.54×10^{-5} (3.54×10^{-5})	4.98×10^{-5} (4.98×10^{-5})	9.66×10^{-5} (9.66×10^{-5})
Equilibrium conversion	50.47% (50%)	38.6% (39.6%)	6.30% (6.4%)
Membrane reactor conversion	69.9% (69%)	56.1% (56%)	27.4 (27%)

rate to a value of 6.7 × 10-8 mole/s instead of 5.8 × 10-8 mole/s. Fitting of the data of Sun et al. (21) required an adjustment of the permeation constant value to a value 1.02×10^{-5} mole/((kPa)$^{0.5}$ s m^2); other parameters were directly extracted from the reported experimental measurements. Fitting of the data by Kokugan et al. (7) required an adjustment of the reaction temperature to a value of 517 K where the reported temperature in the experiments was 473 K and the remaining experimental parameters were extracted from their study.

CONCLUSIONS

Catalytic membrane reactors provide an efficient mean for increasing the reaction conversion through selective permeation for part of the reaction products. This in turn shifts the reaction equilibrium to higher conversion. Conventionally, low conversion reactions are associated with large size fixed bed reactors together with extensive down-stream separation units that recover and recycle un-reacted feed. The main attractive feature of the membrane reactor is the possibilities of replacing many of the conventional separation units and recycling devices with a shell and tube membrane reactor or conventional fixed bed reactor together with membrane separation units. The results and analysis presented here for cyclohexane dehydrogenation in a membrane reactor show conversion sensitivity to variations in the inlet flow rate, heating load, sweep flow rate, cyclohexane mole fraction in the feed stream, permeation constant, shell pressure, feed temperature, and tube diameter. Also, the outlet temperature is found to be sensitive for variations in the heating load and the feed temperature. Analysis shows that the co-current flow mode is more efficient than the counter current flow mode.

SYMBOLS

Cp	Specific heat at constant pressure, kJ/mole K
D	Tube diameter, m
F	Molar flow rate on the tube side, mole/s
G	Molar flow rate on the shell side, mole/s
ΔH	Heat of reaction, kJ/mole
k	Rate constant, mole/(kPa m^3 s)
K_B	Adsorption rate constant of benzene, (Pa^{-1})
K_p	The equilibrium constant of the reaction, (Pa^3)
p	Partial pressure of species i, kPa
q	Heating load, kW/m^3
r_C	Reaction rate of Cyclohexane, mole/s m^3
T	Reaction temperature, K
V	Reactor or tube volume, m^3

Greek Symbols

α_H	Hydrogen permeability, mole/((kPa)$^{0.5}$ s m^2)
δ	Effective membrane thickness, m

Subscripts

B	Benzene
C	Cyclohexane
H	Hydrogen
i	Species (i)
o	Inlet conditions
t	Tube side
s	Shell side

REFERENCES

1. Itoh, N. (1987) A membrane reactor using palladium. *AIChE J*, 33 (9): 1576.
2. Itoh, N., Shindo, Y., Haraya, K., and Hakuta, T. (1988) A membrane reactor using microporous glass for shifting equilibrium of cyclohexane dehydrogenation. *J. Chem. Eng. Jpn.*, 21 (4): 399.
3. Itoh, N. and Wu, T. (1997) An adiabatic type of palladium membrane reactor for coupling endothermic and exothermic reactions. *J. Membr. Sci.*, 124 (2): 213.
4. Itoh, N., Tamura, E., Hara, S., Takahashi, T., Shono, A., Satoh, K., and Namba, T. (2003) Hydrogen recovery from cyclohexane as a chemical hydrogen carrier using a palladium membrane reactor. *Catal. Today*, 82 (1–4): 119.
5. Okubo, T., Haruta, K., Kusakabe, K., Morooka, S., Anzai, H., and Akiyama, S. (1991) Equilibrium shift of dehydrogenation at short space-time with hollow fiber ceramic membrane. *Ind. Eng. Chem. Res.*, 30 (4): 614.
6. Jeong, B., Sotowa, K., and Kusakabe, K. (2003) Catalytic dehydrogenation of cyclohexane in an FAU-type zeolite membrane reactor. *J. Membr. Sci.*, 224 (1–2): 151.
7. Kokugan, T., Trianto, A., and Takeda, H. (1998) Dehydrogenation of pure cyclohexane in the membrane reactor and prediction of conversion by pseudo equilibrium model. *J. of Chem. Eng. Jpn.*, 31 (4): 598.
8. Tiscareño-Lechuga, F., Hill, C.G., Jr., and Anderson, M.A. (1996) Effect of dilution in the experimental dehydrogenation of cyclohexane in hybrid membrane reactors. *J. Membr. Sci.*, 118 (1): 85.
9. Ettouney, H.M., Masiar, B., Bouhamra, W.S., and Hughes, R. (1996) High temperature co shift conversion (HTSC) using catalytic membrane reactors. *Trans IChemE*, 74 (a): 649.
10. Abdalla, B.K. and Elnashaie, S.S.E.H. (1994) Catalytic dehydrogenation of ethylbenzene to styrene in membrane reactors. *AIChE J.*, 40 (12): 2055.
11. Abashar, M.E.E., AlHumaizi, K.I., and Adris, A.M. (2003) Investigation of methane-steam reforming in fluidized bed membrane reactors. *Trans IChemE*, 81 (a2): 251.

12. Ciavarella, P., Casanave, D., Moueddeb, H., Miachon, S., Fiaty, K., and Dalmon, J.A. (2001) Isobutane dehydrogenation in a membrane reactor Influence of the operating conditions on the performance. *Catal. Today*, 67 (1–3): 177.
13. Zhu, B., Li, H., and Yang, W. (2003) AgBiVMo oxide catalytic membrane for selective oxidation of propane to acrolein. *Catal. Today*, 82 (1–4): 91.
14. Xue, E. and Ross, J. (2000) The use of membrane reactors for catalytic n-butane oxidation to maleic anhydride with a butane-rich feed. *Catal. Today*, 61 (1–4): 3.
15. Collins, J.P. and Way, J.D. (1994) Catalytic decomposition of ammonia in a membrane reactor. *J. Mem. Sci.*, 96 (3): 259.
16. Chan, P.P. Y., Vanidjee, K., Adesina, A.A., and Rogers, P.L. (2000) Modeling and simulation of non-isothermal catalytic packed bed membrane reactor for H_2S decomposition. *Catal. Today*, 63 (2–4): 379.
17. Gobina, E. and Hughes, R. (1994) Ethane dehydrogenation using a high-temperature catalytic membrane reactor. *J. Mem. Sci.*, 90 (1–2): 11.
18. Sousa, J.M. and Mendes, A. (2004) Simulating catalytic membrane reactors using orthogonal collocation with spatial coordinates transformation. *J. Mem. Sci.*, 243 (1–2): 283.
19. Abashar, M.E.E. and Al-Rabiah, A.A. (2005) Production of ethylene and cyclohexane in a catalytic membrane reactor. *Chem. Eng. Proc.*, 44 (11): 1188.
20. Koukou, M.K., Chaloulou, G., Papayannakos, N., and Markatos, N.C. (1997) Mathematical modeling of the performance of non-isothermal membrane reactors. *Int. J. Heat Mass Trans.*, 40 (10): 2407.
21. Sun, Y.M. and Khang, S.J.K. (1988) Catalytic membrane for simultaneous chemical reaction and separation applied to a dehydrogenation reaction. *Ind. Eng. Chem. Res.*, 27 (7): 1136.